ELSEVIER

Journal of Nuclear Materials 294 (2001) 32–38

journal of nuclear materials

www.elsevier.nl/locate/jnucmat

A qualitative comparison of barium behaviour in the PHEBUS FPT0 test and analytical tests

R. Dubourg *, P. Taylor [1]

Institut de Protection et de Sûreté, Nucléaire, Département de Recherches en Sécurité, CEA/Cadarache, France

Abstract

Thermochemical considerations have been used to understand the difference between the barium releases observed in the PHEBUS FPT0 in-reactor severe accident test (<1%) and those observed in the ORNL and VERCORS analytical experiments (>40%). BaO is slightly soluble in UO_2, and $BaUO_3$ may also be formed as a separate phase, as may $BaZrO_3$ and more complex solid-solution phases. Barium vapour pressure is generally a monotonic function of the mole fraction of BaO in the fuel; however, the Ba vapour pressure decreases in the region between the solidus and the liquidus, because of a simultaneous decrease of Ba concentration in both liquid and solid phases. Zirconium and iron can also reduce the Ba volatility. These phenomena may be used to rationalize the low release of Ba observed in the PHEBUS FPT0 experiment. © 2001 Published by Elsevier Science B.V.

1. Introduction

Both large-scale integrated tests (such as the PHEBUS FPT series [1]) and smaller-scale analytical or 'separate effects tests (such as the VERCORS series [2,3]) are used to understand the release of fission products (FPs) from fuel under postulated severe accident conditions [4,5]. The aim of this paper is to try to correlate some general properties of barium with the experimental results of PHEBUS FPT0 and VERCORS tests and to rationalise, as far as possible, the differences observed for barium release in these two kinds of experiments.

In the FPT0 test, the maximum temperature before collapse of the fuel assembly was about 2500 K [6]. This is comparable to the maximum temperature plateau of 2570 K achieved in the VERCORS tests. The barium release in PHEBUS FPT0 was very low (<1%), whereas that in VERCORS was high (80% for reducing conditions in VERCORS 4 and 55% for steam conditions in VERCORS 5). The low release in FPT0 is confirmed by the results of the FPT1 test, which was performed under the same conditions but with a higher burnup fuel. The significant difference between in-pile and out-of-pile test results generates important questions related to source-term evaluation and also the calculation of the corium residual power.

We present here a discussion of several factors that can influence the barium behaviour. These factors were identified either from general knowledge of barium properties or thermochemical results. An application of all these factors to the FPT0 test is proposed.

2. Some previous hypotheses

One suggested explanation for the big difference between VERCORS and FPT0 results was the possible existence of a reducing atmosphere in all the VERCORS tests, due to unexpected oxidation of the tungsten susceptor. This atmosphere would have led to the formation of a metallic form of barium in the condensed phase, which would be more volatile than the oxide form BaO. This hypothesis has been rejected mainly because the results of analytical tests are very consistent. This point is illustrated in Table 1, which presents the main results of barium release in HEVA-VERCORS tests

---

* Corresponding author. Tel.: +33-4 42 25 65 13; fax: +33-4 42 25 63 99.

E-mail address: dubourg@sand.cad.cea.fr (R. Dubourg).

[1] Present address: P.O Box 597, Pinawa, Manitoba R0E 1L0, Canada.

0022-3115/01/$ - see front matter © 2001 Published by Elsevier Science B.V.
PII: S0022-3115(01)00471-8

Table 1
Conditions and Ba release data for ORNL (HI and VI) and IPSN tests (HE, VE, HT)

Test No.	Temperature (K)	Duration (min)	Atmosphere	Ba release(%)
HI 4	2200	20	H_2O	<1
HI 5	2025	23	H_2O	<1
VI 2	2300	60	H_2O	19
VI 3	2700	20	H_2O	30
VI 4	2440	20	H_2	27
VI 5	2720	20	H_2	76
HE 4	2270	7	$H_2O + H_2$	6
HE 6b	2370	30	H_2	27
VE 1	2130	17	$H_2O + H_2$	4
VE 4	2570	30	H_2	80
VE 5	2570	30	H_2O	55
HT 1	3070	7	H_2	49

(HE, VE, and HT series [2,3,7]) and corresponding ORNL tests (HI and VI series [8]). The overall results were rather similar in the two series, with no significant Ba release below 2200 K. There is a suggestion of a peak near 2700 K in all atmospheres. Ba release was only slightly sensitive to change of atmosphere, but was somewhat higher in H_2 atmosphere (comparing VERCORS 4 and 5 or VI 5 and 3). We note that there is some uncertainty in the oxygen potential of the fuel in these tests, due to significant flow by-pass).

3. General properties of barium

Concerning their behaviour in the solid phase, the less volatile FPs are currently divided into two broad categories [9], depending on their ability to form oxides, as a function of oxygen potential:

- The five noble metals (Pd, Rh, Ru, Tc, and a portion of the Mo) form metallic inclusions at grain boundaries.
- More reactive metals form oxides, either in solution within the fuel matrix or segregated on the grain boundaries.

The $BaO–UO_2$ pseudobinary phase diagram proposed by Adamson et al. [10] indicates that $BaUO_3$ melts congruently at ~2723 K, and that it coexists with UO_2 up to a eutectic temperature of 2388 ± 40 K. Kleykamp [11] has shown that BaO is slightly soluble (<1 mol%) in UO_2. The phase diagram we discuss below was derived from the Thermodata database, and is consistent with these two references. High barium concentrations, representing medium to high-burnup conditions, may exceed the solubility of BaO in UO_2 and hence $BaUO_3$ can be formed; however, this situation is complicated by other fission products, especially zirconium, which is of course present in fuel cladding as well.

Various reports differ as to the stability of $BaZrO_3$ [9,10,12], but the careful study by Adamson et al. [10] indicates that it melts congruently at 2978 K and that it is compatible with UO_2 (with some mutual solubility) up to a eutectic temperature of 2569 ± 30 K. Furthermore, small quantities of Cs, Sr, U, Pu, Mo and rare earths (RE) can coprecipitate from fuel with Ba and Zr to form a complex solid solution [9], sometimes referred to as the 'grey phase', with the following formula:

$$(Ba_{1-x-y}, Sr_x, Cs_y)(Zr,\ U,\ Pu,\ Mo,\ RE)O_3.$$

It is likely that parts of the following discussion of Ba volatility in the $BaO–UO_2$ system are valid only for low-burnup fuels (such as the trace-irradiated fuel in PHEBUS FPT0), and that the grey phase becomes a complicating factor in medium- and high-burnup fuels. Nevertheless, the calculations for the $BaO–UO_2$ pseudobinary reveal an unusual, somewhat counter-intuitive, temperature dependence of Ba volatility in the solidus–liquidus region.

The volatility of barium has been studied using the Thermodata code GEMINI2, using the TDBCR981 database [13], in the range 1500–3000 K. The volatilisation of Ba can be modelled by considering no change in the oxidation state of Ba, that is to say, by considering an equilibrium between BaO in the condensed phase and in the adjacent gas phase (reaction (1)). Several redox and hydration equilibria are then considered to take into account the gas–phase chemistry (reactions (2)–(4)).

$$\text{Condensed phase I} \leftrightarrow BaO(g) + \text{condensed phase II} \quad (1)$$

$$BaO(g) + H_2O \leftrightarrow Ba(OH)_2(g) \quad (2)$$

$$BaO(g) + H_2 \leftrightarrow Ba(g) + H_2O \quad (3)$$

$$BaO(g) + 1/2H_2 \leftrightarrow Ba(OH)(g). \quad (4)$$

The most important conclusions from this study are the following:

- Ba vapour pressure is a linear function of the mole fraction in the condensed phase except above ~0.5% of Ba (due to the formation of the $BaUO_3$ phase).

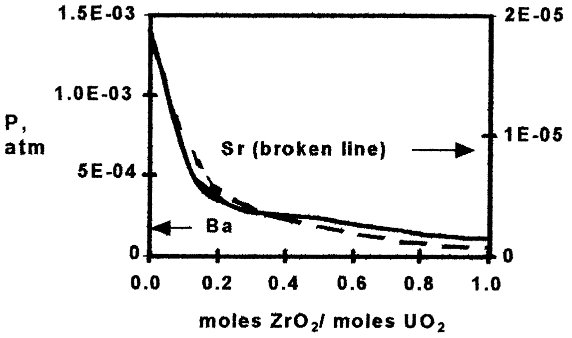

Fig. 1. Partial pressures of Ba and Sr over MO–UO_2–ZrO_2 systems at 2573 K as a function of ZrO_2 : UO_2 molar ratios.

- The overall impact of gas–phase chemistry on Ba volatility is rather small. At high temperatures the hydroxide species become less stable and, for a given H_2/H_2O ratio, Ba(g) becomes more stable with respect to BaO(g).
- The presence of Zr has a great impact on the Ba volatility due to non-ideal behaviour (GEMINI2) or the formation of $BaZrO_3$ (depending on its stability). Fig. 1 shows that at 2573 K, 20% of ZrO_2 in UO_2 can decrease the vapour pressure of barium by about a factor of 10, but the major effect is near 2900 K.
- The vapour pressure of barium over BaO–UO_2 mixtures begins to decrease significantly above ~2600–2700 K under various conditions.

This last important point has been investigated further using thermochemical calculations with the GEMINI2 code. reaction (1) represents situations where a pair of condensed phases (either two solids or a solid and a liquid) control the vaporisation of BaO, in accordance with the Phase Rule.[2] These situations exist at temperatures below the liquidus and compositions outside the solid-solution composition range.[3] Below the solidus, condensed phase I is $BaUO_3(s)$ and condensed phase II is the saturated solid-solution. Above the solidus but below the liquidus, condensed phase I is a liquid phase and condensed phase II is again the saturated solid-solution.

The BaO/UO_2 molar ratios of 0.001 and 0.01 chosen for the current calculations bracket the values used previously to represent the VERCORS tests ($BaO/UO_2 = 0.0024$). For the compositions with the higher Ba concentrations, calculations were based on 1 mol of UO_2 and 1 mol of gas; for those with lower Ba concentrations, the proportions were 1 mol of UO_2 and 0.1 mol of gas. Calculations were performed with four different atmospheres: argon, hydrogen, steam, and 50–50 hydrogen/steam (initial compositions) for the temperature range 1900–2900 K. The limit of 2900 K was chosen because $Ba(OH)_2(g)$ was not available in the TDBCR981 database for GEMINI2 at $T \geqslant 3000.0$ K.

Fig. 2 shows calculations of total barium vapour pressure for the two different Ba concentrations and the four different atmospheres. Examination of the vapour-phase speciation showed that Ba(g) and BaOH(g) were the most important species in a hydrogen atmosphere, whereas $Ba(OH)_2(g)$ and BaOH(g) predominated in steam-containing atmospheres, the former being most important at the lower temperatures. The species BaH(g) and $Ba_2O(g)$ made minimal contributions to barium volatility under all of the conditions examined.

In the calculations with 1% BaO, we can observe a slow increase followed by a maximum in the vapour pressure curves at about 2400 K. This corresponds to the solidus temperature, above which the equilibrium condensed phases change from $[BaUO_3 + (Ba,U)O_2]$ to $[\text{Liquid} + (Ba,U)O_2]$. The modification in the barium volatility appears to be associated with this phase change and the subsequent evolution of the phase compositions between the solidus and the liquidus.

In order to understand more fully the significance of the calculated change in barium volatility above the solidus, it is desirable to extend the calculations

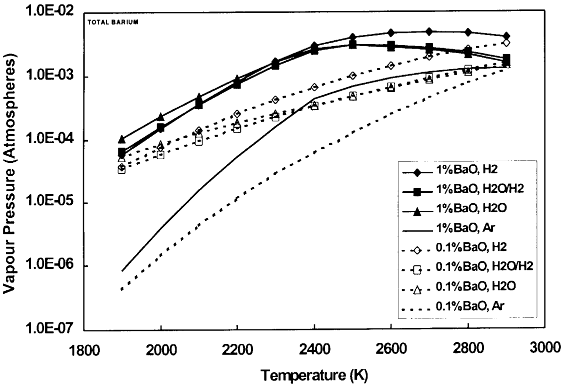

Fig. 2. Ba vapour pressure over UO_2–0.1% BaO and UO_2–1.0% BaO in various atmospheres at 1900–2900 K.

---

[2] According to the Phase Rule, for a system of C components containing P phases, the number of degrees of freedom (including temperature and pressure) is given by $F = C - P + 2$. If we consider the system BaO–UO_2 as a binary system ($C = 2$; see Footnote 3), then in a situation with three phases (two condensed phases and vapour), $F = 1$. Thus, the vapour composition (and hence, the partial pressure of BaO as defined by reaction (1)) varies uniquely with temperature at constant pressure.

[3] Strictly speaking, the O:M ratio of the $(Ba_xU_{1-x})O_{2\pm y}$ solid solution can vary with oxygen potential. GEMINI2 appears to treat the solid solution as a pseudobinary phase, $(BaO)_x(UO_2)_{1-x}$. In this paper, except when specific compositions are being considered, this phase is simply denoted by $(Ba,U)O_2$.

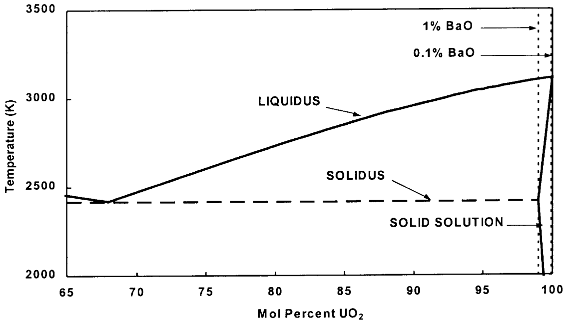

Fig. 3. Solidus–liquidus region of the high-UO_2 portion of the BaO–UO_2 phase diagram. This figure is derived from the Thermodata database.

throughout the two-phase region, i.e., extending to (and above) the liquidus. Because of limitations in the database (in particular, the absence of the $Ba(OH)_2(g)$ species at $T > 3000$ K), these calculations were limited to vaporisation of Ba–U–O compositions in argon. It is useful to consider the BaO–UO_2 pseudobinary [4] phase diagrams in some detail. Fig. 3 shows the solidus/liquidus region of the UO_2-rich portion of the BaO–UO_2 phase diagram. Fig. 4 is a schematic diagram illustrating the melting (and by extension, vaporisation) behaviour of BaO–UO_2 compositions at very low BaO concentrations. Point A represents the melting point of UO_2, B is the eutectic, and C represents the maximum solubility of BaO in UO_2, at the eutectic temperature. The lines BECJA and BJ′FKA represent the solidus (below which all condensed phases are solid) and the liquidus (above which all condensed phases are liquid), respectively.

Line DEFG in Fig. 4 represents the process of heating a composition outside the solid-solution phase field from below the solidus to above the liquidus. Below the solidus (DE), the equilibrium solid phases are the two solids ($BaUO_3$ and $(Ba,U)O_2$ solid solution). On passing to a point just above the solidus (E), partial melting occurs: the BaO-rich solid phase $BaUO_3$ disappears and is replaced by a small quantity of liquid phase with the eutectic composition. To obtain this composition, some dissolution of the solid-solution occurs. As the temperature increases, and one traverses the region between the solidus and the liquidus (line EF), *the compositions of both phases become more dilute in barium* (*and hence one might expect that the barium activity diminishes*), *while the relative quantities of the two phases change* (*increasing amount of liquid relative to solid*). Eventually, at the liquidus (F), the solid phase disappears and at higher temperatures (FG) only the liquid exists.

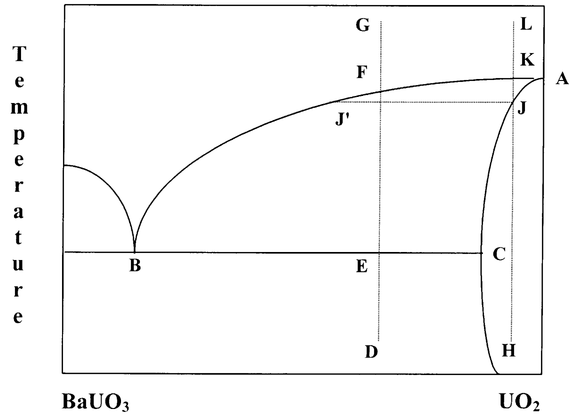

Fig. 4. Representation of solidus–liquidus region in the BaO–UO_2 phase diagram.

Line HJKL in Fig. 4 represents a similar process with a composition that lies within the solid-solution phase field. The situation is parallel to that described above, except that the solidus line is crossed (J) at a higher temperature than the eutectic. The initial liquid composition corresponds to the point J'; the compositions and proportions of the liquid and solid phases evolve between points J and K in a similar manner to that described above for the interval EF.

Fig. 5 shows the calculated Ba(total) and U(total) vapour pressures over $UO_2 - 0.1\%$ BaO and $UO_2 - 1.0\%$ BaO at 2000–3500 K. The variation of the Ba vapour pressure is consistent with the foregoing discussion. For the 1.0% BaO composition, the vapour-pressure curve shows a deviation at the solidus (near 2400 K), declines to a minimum near the liquidus (near 3200 K), then increases monotonically again at higher temperatures. For the 0.1% BaO composition, there is a sharper inflection between 2900 and 3200 K because the solidus temperature is markedly higher in this case (see

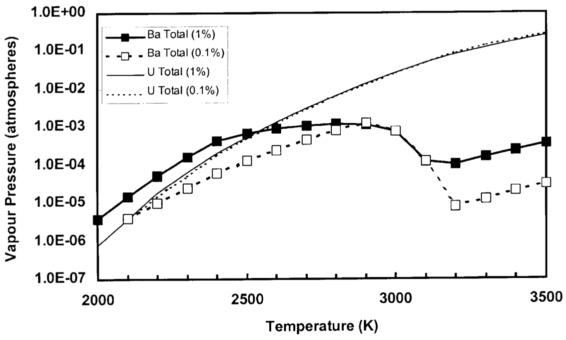

Fig. 5. Calculated vapour pressures (sum of all species) of Ba and U over $UO_2 - 0.1\%$ BaO and $UO_2 - 1.0\%$ BaO in argon atmosphere at 2000–3500 K.

---

[4] i.e., ignoring oxygen potential as a variable; see Footnote 3.

Figs. 3 and 4). In contrast with barium, the uranium vapour pressure increases normally with increasing temperature, and is not markedly different from pure UO_2, as expected.

4. Brief description of the degradation scenario in PHEBUS FPT0 test

We can extract the following main points from [6]. The experimental sequence is divided into different phases.

The first is the calibration phase up to 10 000 s. During this phase, the cladding rupture was detected at about 6960 s corresponding to a maximum temperature of ~1000 K measured at an elevation of 400 mm.

The phase of the control-rod failure corresponds to the period 10 000–11 000 s of the sequence (near 1500 K at the 500 mm elevation) and all the calculations performed (with some limitations) show that after 12 000 s the Ag–In–Cd alloy accumulates near the bottom of the bundle. The understanding of control-rod degradation and the interaction with fuel liquefaction and degradation could be important in the interpretation of the barium release. The situation in FPT0 seems to be complex.

The post-test examination of the re-frozen molten pool at 256 mm showed no trace of Ag–In–Cd. An examination of a slice of the control rod at 67 mm (including a part of the intact cladding and a relocated ‘metallic looking’ material) shows that there is a good correlation between zirconium and iron and also between silver and indium, but a weak correlation between silver and zirconium. On the other hand, other observations have shown the existence of a relocated ceramic material (U–O–Zr) with no silver or indium, and therefore Zr seems to be the only primary solvent for UO_2.

The oxidation period between 11 000 and 12 500 s is the third phase to be considered. In this time interval, 70% of the Zircaloy inventory was consumed and there was a rapid (<500 s) temperature escalation after 12 000 s. During this time, the temperature in the upper part of the bundle (>500 mm) rose very quickly up to 2700 K. In this part of the bundle and during this escalation, it is almost certain that some fuel liquefaction (and relocation) occurred due to interaction with non-oxidised zircaloy or melted stainless steel present in the bundle. Some traces of iron oxide (~1%) were found in molten materials present in the grain boundaries of the intact part of this zone. Most probably, the melting temperature was 2670 K and the melt composition was about 85% UO_2 and 15% Zr(O). In the lower part of the bundle (>500 mm), the oxidation was much less violent.

A very important phase is the ‘collapsing’ phase between 13 000 and 16 000 s that occurs after complete clad oxidation and when the fuel is still largely intact (except for control rod rupture and some relocation during the oxidation phase). Several fuel relocation events have been identified at 14 350, 14 730, 15 180, 15 700 and 16 200 s. The collapsing phase is very difficult to understand, and three scenarios are possible. The most probable is that during the oxidation escalation, some material was relocated from the upper part of the bundle to the 400–500 mm level where it remained solid until 14 000 s. Then it melted again progressively (3 events up to 15 000 s) and fell onto the lower spacer grid. A molten pool was formed between 15 200 and 16 200 s. It is very likely that the relocated materials were $(U, Zr)O_2$ ceramic melts rather than UO_2 fuel pellet fragments.

The last important phase is from 15 000 s to the end of the experiment, and is associated with the formation of a molten pool at the 200–300 mm elevation. The post-irradiation analysis of the frozen melt showed a rather uniform ceramic melt with the composition (mol%) $53UO_2 - 47ZrO_2$ with small amounts of transition metal (Fe, Ni, Cr) oxides (0.5–1 wt%) [14].

By comparison with PHEBUS FPT0, the situation in the VERCORS 4 and 5 tests is very simple. First the experimental scenario is simpler with an oxidation phase of one hour at 1770 K in a mixed steam–H_2 atmosphere, followed by a rather rapid increase to the high-temperature plateau (2570 K), which was maintained for 30 min in a purely reducing (H_2) atmosphere in VERCORS 4 and pure steam atmosphere in VERCORS 5. In both tests a significant degree of fuel degradation occurred (especially in VERCORS 4), but the geometry remained largely intact. Post-test examinations revealed highly porous and cracked pellets and an open and completely oxidised cladding. The fuel had a ‘foamy’ structure, due to copious release of fission gases. It is important to note that, only in VERCORS 5, there was a strong fuel-clad interaction in a 1 mm zone in the external part of the fuel.

5. Discussion

In the VERCORS tests the experimental results are well reproduced by simple models like those of ELSA for semi-volatile species [15] or by thermochemical calculations using GEMINI2 [16]. Regarding the modelling of ELSA, the release of barium in VERCORS can be described by the limiting phenomenon (evaporation-mass transfer) used in this model. In this case diffusion inside the grain is far more rapid than evaporation of barium in the fuel pores and the subsequent mass transfer (or transport) in these pores and the bulk.

Simple thermochemical equilibrium calculations agree well with the VERCORS experimental results [16]. For the temperatures of VERCORS tests, GEMINI2 gave rather similar results for barium evaporation in reducing and steam atmospheres. Apart from the limitations of the GEMINI tool and the limiting necessary hypothesis used in [16], one reason for the difference between VERCORS 4 and 5 may be the strong fuel-clad interaction in VERCORS 5, which could have reduced the vapour pressure of barium by introducing some Zr to the fuel matrix.

In PHEBUS FPT0, the situation is much more complicated. The scenario is different because the rise of temperature is rapid (and there is an escalation due to clad oxidation) and also because earlier interactions led to significant early degradation without high-temperature plateaus, comparable to those in the VERCORS tests. Instead of that, a molten pool, with high temperatures (>3000 K), was formed in the bottom of the bundle in the last phase of the experiment.

Prior to the clad oxidation, the temperature of the bundle was too low (<1700 K) to produce any significant release of barium. During the temperature escalation phase, some interactions occurred.

The temperature escalation caused by clad oxidation was probably too short lived for significant release, but was able to produce melting of the stainless steel present in the bundle, leading to the presence of some iron in the fuel matrix (around 2% in the grain boundary regions as discussed above). This melted stainless steel could have led to early dissolution of Zircaloy cladding of the fuel rods. In turn, this could have caused early formation of barium zirconates in the fuel matrix, or the simple mixing of Zr in the fuel matrix, which can decrease the vapour pressure of barium.

We have tested the impact of adding small quantities (1 mol%) of iron oxide (FeO) to the fuel matrix on the volatility of barium. The result, as given by GEMINI2 with associated validity, is represented in Fig. 6. Without iron, the situation corresponds exactly to the description given in Section 3, that is to say that above ~1500 K (for 0.1 mol% BaO), BaO is miscible in the UO_2 matrix up to the temperature corresponding to the beginning of the transition zone between solidus and liquidus, which is associated with a decrease of the calculated vapour pressure of barium. With 1 mol% FeO, we note that a liquid phase is formed at much lower temperatures (near 1700 K) and that the vapour pressure of barium is reduced by a factor of about 8 in the 2000–3000 K temperature range. This can be attributed to a strong partitioning of barium from the UO_2 solid-solution phase into a small quantity of FeO-rich liquid.

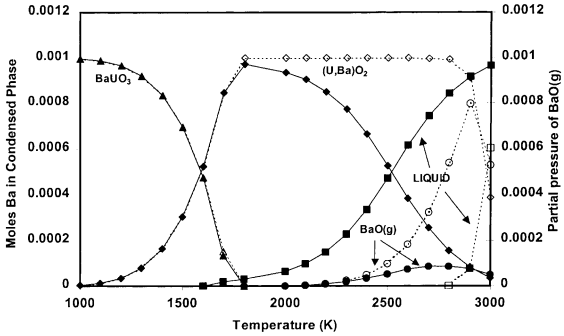

Fig. 6. Calculated distribution of barium between solid $BaUO_3$ (triangle symbols), solid solution (diamonds), liquid (squares) and gas phase (circles) for 1 mol UO_2–0.1% BaO + 1 mol argon at 1000–3000 K. Solid lines and symbols show results with 1 mol% FeO added to the UO_2–0.1% BaO; broken lines and open symbols show results without FeO.

At this point we can conclude that in the PHEBUS FPT0 test prior to any significant relocation, barium release was low due to low temperature, Zr mixing in the fuel matrix, small amounts of iron, and the short duration of temperature escalation. The relocated materials accumulated in a zone where the temperature was first rather low, then increased rapidly to high values with the formation of a molten pool. There was no 'high temperature plateau' as in the analytical tests (ORNL and VERCORS). Subsequently, in the molten pool phase, several factors could have contributed to a low release of barium:

- The effect of the solidus–liquidus transition zone in the U–Ba–O phase diagram.
- The significant amount of ZrO_2 (about 47 mol% in the fuel melt), which can greatly reduce the volatility of barium.
- The small concentrations of iron oxide (and perhaps other oxides).

6. Conclusion

The above discussion provides a basis for interpretation of the significant differences in the barium release observed in complex integrated experiments, like the PHEBUS FPT0 test, and simple analytical experiments like those in the ORNL and VERCORS programs. The main phenomena contributing to a low Ba release in the PHEBUS FPT0 test are reductions in the total Ba vapour pressure (1) in the solidus–liquidus transition zone in the U–Ba–O phase diagram (~2400–3100 K), and (2) due to interactions with iron and zirconium oxides. Only a qualitative interpretation can be proposed at this time, because a detailed description of the bundle degradation scenario would be required to perform quantitative calculations.

References

[1] M. Schwarz, G. Hache, P. von der Hardt, Nucl. Eng. Des. 187 (1999) 47.

[2] B. Andre, G. Ducros, J.P. Leveque, D. Maro, M.F. Osborne, R.A. Lorenz, Nucl. Technol. 114 (1996) 23.

[3] G. Ducros, P.P. Malgouyres, M. Kissane, D. Boulaud and M. Durin, Fission product release and fuel behaviour under severe accidental conditions: Synthesis of the VERCORS 1–6 experimental program, in: International Topic Meeting on Light Water Reactor Fuel Performance, Park City, Utah, 10–13 April 2000, p. 1100.

[4] B.J. Lewis, B.J. Corse, W.T. Thompson, M.H. Kaye, F.C. Iglesias, P. Elder, R. Dickson, Z. Liu, J. Nucl. Mater. 252 (1998) 235.

[5] F.C. Iglesias, B.J. Lewis, P.J. Reid, P. Elder, J. Nucl. Mater. 270 (1999) 21.

[6] M. Schwarz, B. Clément, C. Ktorza, A.V. Jones and R. Zeyen, The PHEBUS FP international research program on severe accidents: status and main findings, in: 26th Water Reactor Safety Meeting, Bethesda, MD, 26–28 October 1998.

[7] G. Ducros, private communication.

[8] M.F. Osborne, R.A. Lorenz, Nucl. Safety 33 (1992) 344.

[9] H. Kleykamp, J. Nucl. Mater. 131 (1985) 221.

[10] M.G. Adamson, E.A. Aitken, R.W. Caputi, J. Nucl. Mater. 130 (1985) 349.

[11] H. Kleykamp, J. Nucl. Mater. 206 (1993) 82.

[12] M. Koizumi, M. Satoh, K. Noro, J. Nucl. Mater. 51 (1974) 90.

[13] P.Y. Chevalier, E. Fischer, B. Cheynet, A. Rivet, G. Cénérino, J. Chim. Phys. 94 (1997) 849.

[14] P.D.W. Bottomley, A.D. Stalios, J.-P. Glatz, B. Satmark, C.T. Walker, J. Nucl. Mater. 278 (2000) 136.

[15] M. Notley, H. Manenc, ELSA: a simplified code for fission products calculation ANS/ENS Conference, Washington, November 1998.

[16] K. Froment, J.M. Seiler, F. Defoort, M. Baichi, G. Ducros, Thermodynamical calculation applied to the fission product release from a degraded fuel pin in VERCORS and VI, CALPHAD XXVIII meeting, Grenoble, May 1999.